Behavioral and Brain Functions

https://doi.org/10.1186/s12993-026-00349-7

Article in Press

Ketamine enhances histone H3 (Ser10) phosphorylation via JNK signaling and multi-omics profiling of the hippocampus in a psychotic-like mouse model

Received: 25 February 2026

Accepted: 17 June 2026

Published online: 25 June 2026

Cite this article as: Zhu X., Li Y., Liu W. *et al.* Ketamine enhances histone H3 (Ser10) phosphorylation via JNK signaling and multi-omics profiling of the hippocampus in a psychotic-like mouse model. *Behav Brain Funct* (2026). https://doi.org/10.1186/s12993-026-00349-7

Xiu-mei Zhu, Yang Li, Wenrui Liu, Ying Pan, Ang Li, Gui-na Han, Jun Yao & Hongbo Wang

We are providing an unedited version of this manuscript to give early access to its findings. Before final publication, the manuscript will undergo further editing. Please note there may be errors present which affect the content, and all legal disclaimers apply.

If this paper is publishing under a Transparent Peer Review model then Peer Review reports will publish with the final article.

ARTICLE IN PRESS

© The Author(s) 2026. **Open Access** This article is licensed under a Creative Commons Attribution-NonCommercial-NoDerivatives 4.0 International License, which permits any non-commercial use, sharing, distribution and reproduction in any medium or format, as long as you give appropriate credit to the original author(s) and the source, provide a link to the Creative Commons licence, and indicate if you modified the licensed material. You do not have permission under this licence to share adapted material derived from this article or parts of it. The images or other third party material in this article are included in the article's Creative Commons licence, unless indicated otherwise in a credit line to the material. If material is not included in the article's Creative Commons licence and your intended use is not permitted by statutory regulation or exceeds the permitted use, you will need to obtain permission directly from the copyright holder. To view a copy of this licence, visit http://creativecommons.org/licenses/by-nc-nd/4.0/.

ARTICLE IN PRESS

Title: Ketamine Enhances Histone H3 (Ser10) Phosphorylation via JNK Signaling and Multi-Omics Profiling of the Hippocampus in a Psychotic-like Mouse Model

Authors: *Xiu-mei Zhu[1,2,3*], Yang Li[4*], Wenrui Liu[5*], Ying Pan[1,2,3], Ang Li[1,2,3], Gui-na Han[6], Jun Yao[1,2,3#], Hongbo Wang[7#].*

Institution:

1. School of Forensic Medicine, China Medical University. Shenyang, P.R. China.

2. Key Laboratory of Forensic Bio-evidence Sciences, Liaoning Province. Shenyang, P.R. China.

3. China Medical University Center of Forensic Investigation. Shenyang, P.R. China.

4. Department of Blood Transfusion, Shengjing Hospital of China Medical University, Shenyang, P.R. China.

5. Central Hospital of Shenyang Sujiatun, Shenyang, P.R. China.

6. Department of Gynaecology, Shenyang Fifth People's Hospital, Shenyang, P.R. China.

7. Department of Human Anatomy, School of Basic Medicine, Shenyang Medical College, Shenyang, P.R. China.

Short title: *ketamine induces transcriptome-wide responses*

Email address: *Xiu-mei Zhu*, 1014124431@qq.com

Yang Li, ly-19870811@163.com

Wenrui Liu, 86262463@qq.com

Ying Pan, 921247280@qq.com

Ang Li, leeang0922@outlook.com

Gui-na Han, 191318092@qq.com

Jun Yao, yaojun198717@163.com

Hongbo Wang, wanghongbo@symc.edu.cn

*: Xiu-mei Zhu, Yang Li, and Wenrui Liu are the co-first authors.

ARTICLE IN PRESS

ARTICLE IN PRESS

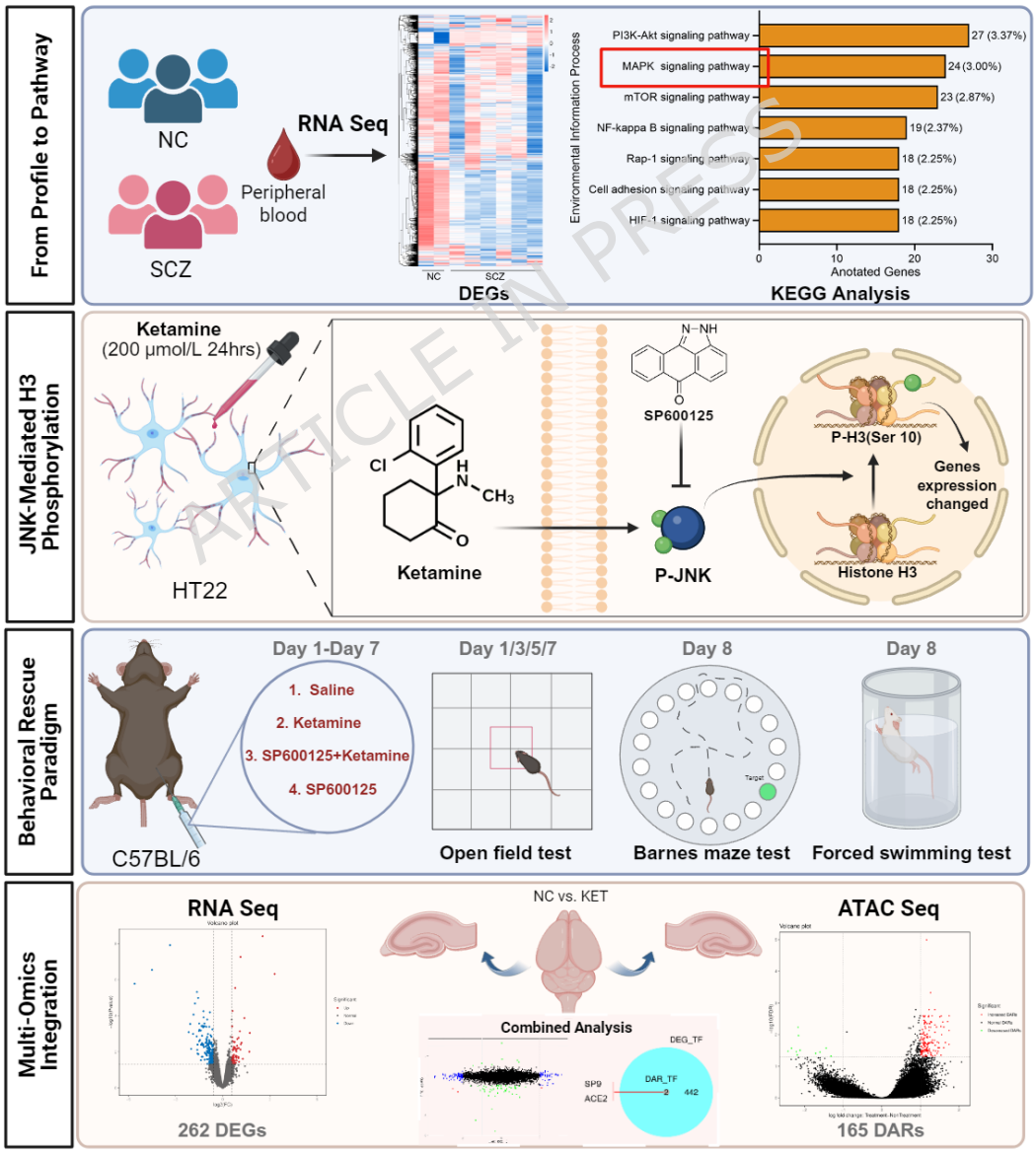
Corresponding authors: *Hongbo Wang and Jun Yao*.

Full postal address of the submitting author: *China Medical University, No.77, Puhe Road, Shenbei New District, Shenyang, 110122, P.R. China.*

Title

Ketamine Enhances Histone H3 (Ser10) Phosphorylation via JNK Signaling and Multi-Omics Profiling of the Hippocampus in a Psychotic-like Mouse Model

Graphic abstract



ARTICLE IN PRESS

Abstract

Ketamine, a dissociative anesthetic, induces behavioral and molecular alterations associated with psychosis-like phenotypes. However, the epigenetic mechanisms bridging its cellular effects with behavioral outcomes are poorly defined. Here, we report that ketamine induces histone H3 Ser10 phosphorylation in both hippocampal neurons (HT22 cells) and the mouse hippocampus, an effect primarily driven by JNK activation. Critically, pharmacological inhibition of JNK with SP600125 not only reversed this epigenetic mark but also robustly attenuated ketamine-induced hyperlocomotion and cognitive deficits in mice. Integrated multi-omics analysis of the hippocampus 30 minutes post-ketamine revealed coordinated transcriptional and chromatin accessibility changes. We identified 262 differentially expressed genes (e.g., MAP3K9) enriched in MAPK signaling and neuroactive ligand-receptor pathways, alongside 165 differentially accessible regions, with motif analysis implicating CTCF as a key regulator. Our findings suggest that JNK-mediated H3S10 phosphorylation may play a critical role in linking ketamine exposure to psychosis-like phenotypes, providing a mechanistic framework that connects stress-sensitive signaling to rapid chromatin remodeling and sustained transcriptional reprogramming. This work unveils potential novel therapeutic targets for psychosis centered on the JNK–H3S10 phosphorylation axis.

Key Words: Ketamine, JNK signaling, MAPK, Histone H3 phosphorylation, Transcriptomics, Chromatin Accessibility.

1. Introduction

ARTICLE IN PRESS

Ketamine, first synthesized in 1962 as a dissociative anesthetic, produces analgesic and dissociative effects through modulating glutamatergic neurotransmission, leading to inhibition of the thalamo-cortical system [1–3]. Controlled administration of ketamine in healthy volunteers leads to positive, negative, and cognitive symptoms similar to those observed in patients with schizophrenia [4]. At sub-anesthetic doses, repeated ketamine administration induces psychotic-like behavioral and neurochemical alterations in rodents, and therefore has been widely employed as a pharmacological model to investigate the pathophysiology of schizophrenia [5,6]. Moreover, positron emission tomography (PET) studies in vivo have demonstrated that sub-chronic ketamine treatment upregulates dopamine synthesis capacity in the midbrain, consistent with the dopaminergic disturbances long recognized in schizophrenia [7,8].

Accumulating evidence highlights the role of the mitogen-activated protein kinase (MAPK) signaling cascade in schizophrenia [9,10]. Schizophrenia-associated genes have been linked to MAPK pathways, and transcriptomic analyses in demyelination and cognitive impairment models reveal enrichment of differential expressed genes in the PI3K–Akt and MAPK cascades [11,12]. Beyond transcriptional regulation, MAPK signaling also influences chromatin structure through histone post-translational modifications (PTM). Phosphorylation of histone H3 at serine 10 or 28, mediated by ERK1/2 and p38, represents a critical nucleosomal activation event. For instance, glutamate stimulation activates ERK and p38, promoting

ARTICLE IN PRESS

H3 (Ser10) phosphorylation (H3S10ph) and driving transcription of immediate-early genes such as c-Fos and c-Jun [13–17]. Dysregulation of this pathway has been linked to hippocampal neurodegeneration and persistent learning and memory deficits following ketamine exposure in rodents [18–20], while elevated H3S10ph has also been observed in peripheral blood mononuclear cells of schizophrenia patients [21]. However, which specific MAPK member mediates ketamine-induced H3S10ph, and whether this signaling axis underlies ketamine's psychotic-like behavioral effects, remain unknown. We therefore hypothesize that aberrant MAPK-H3S10ph signaling represents a mechanistic link between ketamine exposure and psychotic-like phenotypes, and set out to identify the responsible upstream kinase.

In this study, we first examined the induction of H3S10ph and the activation of MAPK family members (JNK, P38, ERK) following ketamine treatment in vitro. To delineate the responsible signaling cascade, we applied pharmacological modulators of MAPK pathways in vitro and identified the specific pathway mediating ketamine-induced H3S10ph, which was subsequently validated in mouse models. Behavioral assessments were then conducted to determine whether this pathway contributes to ketamine-induced psychotic-like phenotypes. Additionally, given our previous finding that ketamine modulates DRD1 expression[22], conditional DRD1 knockout mice were employed as an exploratory approach to assess potential interactions with the identified signaling pathway. Finally, integrated ATAC-seq and RNA-seq analyses were performed to identify transcriptional

ARTICLE IN PRESS

regulators and downstream gene expression changes associated with these pathways.

2. Materials and Methods

2.1. Cell culture

The HT22 mouse hippocampal neural cell line was purchased from Procell Life Science and Technology, Co, Ltd (Wuhan, China). The cells were cultured in DMEM high glucose medium (Viva Cell Bioscience, Shanghai, China) containing 10% fetal bovine serum (Procell Life Science and Technology) and maintained at 37 °C in a 5% CO_2 incubator.

2.2. Cell treatment

When the cell density reached 60%, the cells were incubated in 0, 10, 20, 50, 100, 200, 500, 1000 μmol/L of Ketamine hydrochloride (Fujian Gutian Pharmaceutical Co., Ltd., Gutian, Fujian, P.R. China), 20 μmol/L P38 pathway inhibitor SB203580, 20 μmol/L ERK pathway inhibitor PD98059, 20 μmol/L JNK pathway inhibitor SP600125 or 1 μmol/L P-ERK1/2 agonist Ro67-7476 (MedChem Express, USA) (Table 1). The detailed treatments were shown using the timeline in the following figures and Table 2.

2.3. Animals

The experimental protocol was approved by the Ethics Committee for Animal Experiments of China Medical University. Eight-week-old male C57BL/6 mice were obtained from Huafukang Bio-Technology, Co, Ltd (Beijing, China) and

ARTICLE IN PRESS

were housed in a standard laboratory condition (12-hour light/dark cycle, 22±2 °C, 40–60% humidity) with unrestricted access to food and water. To minimize the impact of environmental change on the behavior, the mice underwent a minimum acclimation period of one week prior to the start of the study.

C57BL/6J-EMX1-Cre$^{+/+}$ mice (Stock No. C001011) and C57BL/6J-DRD1$^{flox/-}$ (Quote:CKOAI211013ZQ1-UP) heterozygous recombinant mice were purchas ed from Cyagen Biosciences Inc, respectively. To delete DRD1 in the cerebr al cortex and hippocampus[23,24], C57BL/6J-DRD1$^{flox/-}$ mice were firstly inter-c rossed to generate homozygous (C57BL/6J-DRD1$^{flox/\ flox}$) mice. Then, C57BL/ 6J-DRD1$^{flox/\ flox}$ mice were crossed with C57BL/6J-EMX1-Cre$^{+/+}$ mice[25] to gen erate mice that are heterozygous for the DRD1 allele and hemizygous/heter ozygous for EMX1-Cre (EMX1-Cre$^{+/-}$; DRD1 $^{flox/-}$ mice). Finally, EMX1-Cre$^{+/-}$; DRD1 $^{flox/-}$ mice were crossed with homozygous C57BL/6J-DRD1$^{flox/\ flox}$ mice to generate targeted EMX1-Cre$^{+/-}$; DRD1 $^{flox/flox}$ mice (DRD1 cKO mice). The genotyping was performed according to the manufacturer's recommendatio ns.

2.4. Drug administration

The C57BL/6 Mice were randomly divided into four groups: saline group (NC group, negative control, n=15), ketamine group (KET group, n = 15), JNK pathway inhibitor + ketamine group (SP600125+KET group, n = 6) and JNK pathway inhibitor group (SP600125 group, n = 6). Of these, 11 NC and 11 KET mice were used as counterparts for the JNK inhibition and DRD1 cKO

ARTICLE IN PRESS

experiments, whereas the remaining 4 NC and 4 KET mice were subjected to hippocampal RNA-seq and ATAC-seq. The cKO mice were randomly divided into two groups: EMX1-Cre$^{+/-}$; DRD1$^{flox/\ flox}$ group (cKO-NC group, n = 5), and EMX1-Cre$^{+/-}$; DRD1$^{flox/\ flox}$ ketamine group (cKO-KET, n = 5). The mice received daily intraperitoneal injections of saline or drugs from 17:00 to 18:00 for seven days. All drugs were diluted in 0.9% saline. The specifics of the drug administration were as follows:

NC group: Mice were injected intraperitoneally with 0.9% NaCl (w/v) solution at a volume of 100 μl/10 g, followed by a second injection of the same dose 30 minutes later.

KET group: Ketamine hydrochloride was dissolved in saline at a concentration of 10 mg/ml. Mice were injected intraperitoneally with 0.9% NaCl (w/v) solution at a volume of 100 μl/10 g. Thirty minutes later, mice were injected intraperitoneally at a volume of 100 μl/10 g with a final ketamine concentration of 100 mg/kg in the mice. The selection of this dosage was according to the previous studies [22,26].

SP600125+KET group: Mice were injected intraperitoneally with SP600125 (HY-12041, MedChemExpress, NJ, USA) at a concentration of 1.5 mg/ml, at an injection volume of 100 μl/10 g. The final concentration of SP600125 in the mice was 15 mg/kg. Thirty minutes after the SP600125 injection, the mice were injected intraperitoneally with ketamine at a concentration of 10 mg/ml, at an injection volume of 100 μl/10 g. The final concentration of ketamine in the mice was 100 mg/kg.

ARTICLE IN PRESS

SP600125 group: Mice were injected intraperitoneally with SP600125 at a concentration of 1.5 mg/ml, at an injection volume of 100 μl/10 g. The final concentration of SP600125 in the mice was 15 mg/kg. Thirty minutes later, mice received an additional intraperitoneal injection of 0.9% NaCl (w/v) solution at the same volume (100 μl/10 g).

cKO-NC group: Mice were injected intraperitoneally with 0.9% NaCl (w/v) solution at a volume of 100 μl/10 g, followed by a second injection of the same dose 30 minutes later.

cKO-KET group: Ketamine hydrochloride was dissolved in saline at a concentration of 10 mg/ml. Mice were injected intraperitoneally at a volume of 100 μl/10 g with a final ketamine concentration of 100 mg/kg in the mice. Thirty minutes later, mice received an additional intraperitoneal injection of 0.9% NaCl (w/v) solution at the same volume (100 μl/10 g).

ARTICLE IN PRESS

2.5. Behavioral tests

Behavior was observed after 30 minutes of daily administration. On day 1, the mice were acclimated to the open field environment. Their autonomous behavior was then evaluated on days 3, 5, and 7. For the Barnes maze test, the mice underwent an acclimatization learning phase from days 3 to 7, followed by the formal evaluation on day 8. The forced swimming test was then conducted six hours after the completion of the Barnes maze evaluation on day 8.

2.5.1 Open field test

The open field test was employed to evaluate the autonomous behavior,

ARTICLE IN PRESS

exploratory behavior, and anxiety levels of mice. This test took place in a white wooden box measuring 40 cm × 40 cm × 30 cm, which was divided into central and surrounding areas. Prior to the experiment, each mouse was given 5 minutes to acclimate to the box. The ALSVision tracking software (AniLab Co., Ltd., Ningbo, Zhejiang, P.R. China) was used to record the total distance traveled and average speed of the mice during the 10-minute experiment. After each mouse finished the experiment, the wooden box was cleaned with 15% alcohol to eliminate any residual odor.

2.5.2. Barnes maze test

The Barnes maze experiment was conducted to assess the spatial memory abilities of mice. The experiment involved the mice escaping from the center of a bright white circular platform (d=92 cm) to a dark box located beneath the platform's edge, known as the target box. The experiment consisted of two phases: an acclimatization learning phase and a formal experimental phase.

ARTICLE IN PRESS

In the acclimatization learning phase, the mice were placed in an opaque container for 30 seconds to adapt to the dark environment in the middle of the platform. After the container was removed, the mice were timed for three minutes. If the mice found the target hole within this time frame, they were allowed to remain in the hole for 30 seconds. Conversely, if the mice failed to locate the target hole within three minutes, they were guided to enter the target hole and stay there for 30 seconds.

The formal experimental phase lasted for one day and involved the use of

ARTICLE IN PRESS

ALSVision tracking software. This software was employed to record the trajectory of the mice as well as the time it took for them to reach the target hole.

2.5.3. Forced swimming test

The forced swimming test has been utilized as an experimental paradigm for evaluating avolition, a key negative symptom of schizophrenia. This test was conducted in a cylinder with a diameter of 10 cm and a depth of 22 cm, filled with water at a temperature of 20–22°C. Each mouse had a total swimming time of 8 minutes, including a 2-minute adaptation period. After the adaptation period, the immobility time for each mouse, the absence of active struggle with the mouse floating in the water, was recorded using SMART™ tracking software (San Diego Instruments, San Diego CA, USA).

2.6. Sample collecting

The cells were collected for western blot analysis or fixed with 4% paraformaldehyde for cellular immunofluorescence after 24 hours of drug treatment. In animal studies, mice were anesthetized with overdose sevoflurane and decapitated on the eighth day after behavioral experiments or 30 minutes following the seventh-day injection. The prefrontal cortex (PFC) and hippocampus of the mice were harvested. The hippocampus of four mice in NC, KET group was used for western blot analysis, RNA sequencing and ATAC sequencing, while the the brain tissue of the other mice in each group was used for western blot analysis.

Peripheral blood samples from six individuals with schizophrenia and two

ARTICLE IN PRESS

healthy individuals were collected from the Mental Health Center of Hanting District, Weifang City, Shandong Province, P.R. China. Informed consent was obtained and the study was approved by the Ethics Committee of Weifang Medical College. The patients were diagnosed according to the *American Diagnostic and Statistical Manual of Mental Disorders* (5th edition). All individuals with schizophrenia met DSM-5 criteria for schizophrenia. The cohort included six individuals (3 males and 3 females; mean age 41.7 ± 3.7 years) presenting with prominent positive symptoms (e.g., auditory hallucinations, persecutory delusions) and negative symptoms (e.g., affective flattening, avolition), with a mean illness duration of 12.8 ± 3.6 years. Blood samples were collected at admission. Healthy controls included two individuals (1 male, 1 female; mean age 41.0 ± 2.8 years) with no personal or family history of psychiatric disorders.

ARTICLE IN PRESS

2.7. Western blot

The cells were washed twice with sterile PBS to remove the medium. NP40, mixed with PMSF (10%, v/v) and phosphatase inhibitors (1%, v/v), was used to extract total proteins from the cells and mice. The protein was quantified using the bicinchoninic acid (BCA) method. Subsequently, the proteins were denatured at 100°C for 5 minutes, separated by SDS-PAGE gel electrophoresis, and transferred to a PVDF membrane using wet transfer at 100V for 1 hour. Following a 3-hour incubation at room temperature with 8% skim milk for blocking, the membranes were incubated overnight at 4°C with the primary antibody at a proper dilution (Table 3). After three washes with

ARTICLE IN PRESS

TBST, the blots were incubated for 2 h with secondary antibody (1:5000, goat anti-rabbit, cat. #A21020, Abbkine, CA, USA; 1:5000, goat anti-mouse, cat. #A21010, Abbkine). The target proteins were detected using an ECL luminescent solution and the Tanon-5500 chemiluminescence imaging analysis system (Tanon, Shanghai, China). The target protein levels of each sample were quantified from the grayscale value using ImageJ software.

2.8. Immunofluorescence

The detail was presented in supplementary material.

2.9. RNA-seq

The detail was presented in supplementary material.

2.10. ATAC-seq

The detail was presented in supplementary material.

2.11. Statistical analysis

All statistical analyses were performed using GraphPad Prism (Ver. 8.0.1). Behavioral test, western blot, and immunofluorescence data are presented as the mean ± standard error of the mean (SEM). A value of $P < 0.05$ was considered statistically significant.

For single-factor experiments involving comparisons with a normalized control value (e.g., k ketamine concentration gradients or single pharmacological treatments in HT22 cells, where the control was set to 1), one-sample t-test was used to determine whether each treatment group mean significantly differed from the theoretical value of 1. This approach was chosen because each gel contained only one NC control, making one-way

ARTICLE IN PRESS

ANOVA with post hoc comparisons inappropriate. Effect sizes (Cohen's d) and degrees of freedom are reported in Supplementary statistical data table. For experiments involving two independent variables (e.g., ketamine × pharmacological inhibitor treatment), two-way ANOVA followed by Sidak's multiple comparisons test was applied. For behavioral assays involving repeated measurements across time, repeated-measures two-way ANOVA followed by Sidak's multiple comparisons test was used.

For immunofluorescence analyses involving multiple groups (eight groups in total), statistical comparisons were performed using one-way ANOVA followed by Tukey's multiple comparisons test.

All statistical data are presented in the Supplementary statistical data table.

3. Results

3.1. Transcriptomic profiling identifies MAPK signaling as a potential regulator associated with schizophrenia

ARTICLE IN PRESS

To explore molecular pathways potentially associated with schizophrenia, we first performed RNA-seq using peripheral blood samples from six individuals with schizophrenia and two healthy controls. Differential expression analysis revealed that the altered genes were significantly enriched in the MAPK and PI3K–Akt signaling pathways (Figure 1a, Figure S1). These findings highlighted MAPK signaling as a potentially important regulatory pathway in schizophrenia-related molecular changes. Guided by this result, we subsequently investigated whether ketamine-induced molecular alterations in our experimental model involved components of the MAPK pathway.

ARTICLE IN PRESS

3.2. Ketamine activates JNK signaling and induces histone H3 Ser10 phosphorylation in HT22 cells

To determine whether ketamine modulates MAPK signaling in neuronal cells, HT22 cells were exposed to increasing concentrations of ketamine for 24 hours. Western blot analysis showed a dose-dependent elevation of p-JNK/JNK and p-H3(Ser10)/H3, with phosphorylation of H3 (Ser10) peaking at 200 μ M ketamine (Figure 1b–1d). In contrast, p-ERK/ERK levels progressively decreased, while p-P38/P38 exhibited only a slight increase. These results indicate that ketamine preferentially activates the JNK pathway and enhances H3 Ser10 phosphorylation, a chromatin mark associated with rapid transcriptional activation.

3.3. Pharmacological dissection identifies JNK as the critical mediator of ketamine-induced H3 Ser10 phosphorylation

To further clarify the contribution of each MAPK subpathway, HT22 cells were pre-treated with specific inhibitors or agonists. The JNK inhibitor SP600125 significantly reduced the p-H3(Ser10)/H3 ratio despite a compensatory decrease in total JNK that elevated the p-JNK/JNK ratio (Figure S2b–c). The ERK inhibitor PD98059 enhanced p-H3(Ser10)/H3, mimicking ketamine’s effect. The P38 inhibitor SB203580 increased p-JNK/JNK and p-H3(Ser10)/H3 without altering P38 phosphorylation (Figure S2b–c). Because ERK inhibition unexpectedly increased H3S10 phosphorylation, an ERK agonist (Ro67-7476) was used for confirmation. ERK activation failed to block ketamine’s effect on H3S10 phosphorylation, whereas SP600125 robustly

ARTICLE IN PRESS

attenuated it (Figure 1e–k). Immunofluorescence further confirmed a significant reduction in ketamine-induced p-H3(Ser10) signals following JNK inhibition (Figure 2a–b).

These findings suggest that JNK activation is a major upstream regulator contributing to ketamine-induced H3S10 phosphorylation.

3.4. JNK inhibition attenuates ketamine-induced psychosis-like behaviors in mice

To examine whether JNK signaling contributes to ketamine-induced behavioral abnormalities, mice were treated with SP600125 and ketamine for seven days. In open field test, ketamine markedly increased total moving distance, movement duration, and center-zone exploration on days1, 3, 5, and 7. SP600125 co-administration significantly reversed these hyperlocomotive and excitatory behaviors (Figure 3b–c). Ketamine impaired spatial learning and memory in Barnes maze, as reflected by longer latency and more errors before locating the target hole. SP600125 significantly ameliorated these deficits, whereas SP600125 alone slightly improved performance relative to controls (Figure 3d–e). No significant differences were observed among the groups in forced swimming test (Figure S2e). Together, these results indicate that JNK inhibition robustly mitigates ketamine-induced locomotor hyperactivity and cognitive impairment, supporting an association between JNK–H3S10 signaling and psychosis-like behavioral alterations.

3.5. JNK pathway inhibition reduces H3 Ser10 phosphorylation and downstream transcription factor activation in the hippocampus

ARTICLE IN PRESS

To connect behavioral changes with molecular alterations in the brain, protein levels were analyzed in the PFC and hippocampus on day 8. Although ketamine induced a nonsignificant upward trend of p-H3(Ser10)/H3 in the PFC, SP600125 markedly reduced p-H3(Ser10)/H3 in both brain regions (Figure 3f–h). Notably, SP600125 also decreased phosphorylation of c-Jun and ATF-2 in hippocampus, two major transcription factors downstream of JNK. The increase of p-MKK4, an upstream kinase of JNK, further confirmed pathway involvement in hippocampus.

Given the transient nature of histone phosphorylation, the modest effect in the hippocampus at day 8 likely reflects a missed detection window. To capture early responses, hippocampal tissue was collected 30 minutes after ketamine injection on day 7 under the same dosage and schedule. Ketamine significantly increased the p-H3(Ser10)/H3 ratio compared to the control group (Figure 3i), indicating rapid induction of hippocampal H3S10 phosphorylation. This effect was blocked by the JNK inhibitor SP600125 (Figure 3f–h), suggesting that ketamine-induced H3S10 phosphorylation is mediated by JNK signaling.

ARTICLE IN PRESS

3.6. Early hippocampal transcriptomic and chromatin changes after ketamine

RNA-seq was performed on hippocampal tissue collected 30 minutes after the final ketamine injection (100 mg/kg, i.p., Day 7; Figure 4a). Differentially expressed genes (DEGs) were defined by |fold change| ≥ 1.5 and $P < 0.05$, yielding 262 DEGs (68 upregulated, 194 downregulated) in the KET group

ARTICLE IN PRESS

relative to NC controls (Figure 4b–c, Table S1). The predominance of downregulated genes suggests that acute ketamine exposure broadly suppresses hippocampal transcriptional activity at this early timepoint. KEGG enrichment analysis of all DEGs highlighted pathways involved in neuroactive ligand–receptor interaction, PI3K-Akt signaling, MAPK signaling, axon guidance, and Alzheimer's disease (Figure 4d, Table S2), consistent with ketamine's known actions on glutamatergic and dopaminergic neurotransmission and its activation of MAPK cascades demonstrated in the preceding experiments. GO molecular function enrichment further identified protein serine/threonine kinase activator activity as a significantly enriched term (Figure S4a), and protein–protein interaction network analysis identified MAP3K9 as a hub node among DEGs (Figure S4b).

Given that H3S10 phosphorylation promotes chromatin remodeling and accessibility during interphase, we performed ATAC-seq on the same hippocampal samples to profile ketamine-induced chromatin accessibility changes. DARs were identified using fold change ≥ 2 and FDR ≤ 0.05 as thresholds, yielding 165 DARs (Figure 5a, Table S3). Genomic annotation revealed that 60.98% of DARs were located in distal intergenic regions, with approximately 10% mapping to promoter-proximal regions (≤ 3 kb from TSS; Figure 5b). KEGG and GO enrichment analyses of genes associated with promoter-proximal DARs highlighted nitrogen metabolism, zinc ion binding, and ATP binding (Figure 5c–d). Motif enrichment analysis of promoter-associated DARs using MEME-CHIP ($P < 0.05$) identified CTCF, CTCFL, and

ARTICLE IN PRESS

ABI4 as the most significantly enriched transcription factor binding motifs (Figure 5e). CTCF motif was associated with DARs annotated to Blcap, Xkr5, Rad51b, and Adgb (Figure 5f).

Circos visualization of paired RNA-seq and ATAC-seq data demonstrated a general correspondence between regions of increased chromatin accessibility and higher gene expression at the chromosomal level (Figure S4c). The nine-quadrant plot showed that the majority of DAR-associated genes did not reach DEG thresholds at this 30-minute timepoint (Figure S4d). Venn diagram analysis identified SP9 and ACE2 as transcription factors present in both the promoter-associated DAR motif enrichment results and the DEG list (Figure S4e).

3.7. Cortical DRD1 deletion modulates ketamine responses

To explore upstream modulators of JNK–H3S10P signaling, EXM1-Cre$^{+/-}$; DRD1^flox/flox mice with cortical excitatory neuron-specific DRD1 deletion were generated. Behaviorally, DRD1 deletion alone increased locomotor activity and Barnes maze latency, while ketamine exposure in cKO mice partially reversed these effects. Molecularly, cKO mice displayed elevated basal p-MKK4, p-P38/P38, and p-H3(Ser10), and ketamine partially reduced these levels without affecting p-c-Jun (Figure S3). These findings suggest that DRD1 may modulate the baseline state of JNK–H3S10P signaling and ketamine responsiveness, rather than serving as a direct upstream driver of this pathway, providing a potential upstream regulatory influence.

4. Discussion

ARTICLE IN PRESS

In this study, we provide evidence that ketamine preferentially activates the JNK pathway in hippocampal neurons, leading to rapid phosphorylation of histone H3 at Ser10 (H3S10ph). RNA-seq analysis of peripheral blood from patients with schizophrenia suggested enrichment of MAPK signaling, which guided our mechanistic exploration. Consistently, in HT22 cells, ketamine induced a dose-dependent increase in p-JNK and H3S10ph, with maximal H3S10 phosphorylation observed at 200 μM. Pharmacological inhibition with SP600125 fully reversed ketamine-induced H3S10ph, supporting JNK as a major upstream regulator contributing to this epigenetic modification. Similarly, in mice, JNK inhibition attenuated ketamine-induced H3S10ph in both the hippocampus and prefrontal cortex, demonstrating the in vivo relevance of this mechanism. Importantly, independent studies have reported alterations in MAPK signaling, including dysregulated JNK-related kinase activity in postmortem prefrontal cortex and increased histone H3 Ser10 phosphorylation in peripheral blood cells of individuals with schizophrenia, indicating that both components of this signaling cascade are individually affected in the clinical condition[21,27].

Although our initial dataset was derived from a small cohort of patients with schizophrenia and cannot be generalized, the enrichment of MAPK signaling is noteworthy. Importantly, this observation converges with larger-scale transcriptomic studies[28] reporting dysregulation of MAPK-related gene networks in schizophrenia, which guided our mechanistic exploration despite the limited sample size. The differences in transcriptomic profiles between

ARTICLE IN PRESS

patients with schizophrenia and ketamine-treated mice likely reflect differences in disease chronicity, experimental paradigm, tissue origin, and species[29,30].

In vitro, exposure of HT22 cells to increasing concentrations of ketamine (0–1000 μM, 24 h) resulted in dose-dependent increases in both JNK and H3S10ph, with H3S10ph peaking at 200 μM. This concentration was therefore selected for subsequent in vitro experiments. Notably, the JNK inhibitor SP600125 fully reversed ketamine-induced H3S10ph in HT22 cells, an effect that was similarly observed in mouse models, further supporting a JNK-dependent contribution to H3S10 phosphorylation. The previous studies similarly reported increased H3S10ph at c-fos and c-jun promoters in formaldehyde-treated lung adenocarcinoma cells through JNK pathway[31]. In addition to formaldehyde, JNK-mediated H3S10ph can also be observed following exposure to carcinogenic stimuli such as cigarette smoke and arsenite[32,33]. JNK has also been shown to promote G2/M entry via H3S10ph, with SP600125 blocking this modification and inhibiting cell cycle progression[34]. Together, these findings suggest that ketamine-induced H3S10ph is JNK-dependent, highlighting JNK's central role in neuronal signaling, epigenetic regulation, and potential pharmacological effects.

Studies have also demonstrated that ketamine and esketamine modulate MAPK signaling in a context-dependent manner. For example, esketamine improves postoperative cognitive dysfunction through the TLR4/MyD88/p38 pathway and reduces neuronal apoptosis via p38 inhibition, whereas

ARTICLE IN PRESS

ketamine has also been shown to downregulate p38 signaling and proinflammatory cytokines [35–37]. Likewise, in the ERK cascade, ketamine upregulates DRD1-ERK-c-Fos signaling in the nucleus accumbens and alters MEK/ERK activation during hypnosis and neuroplasticity [38,39]. In the JNK pathway, ketamine attenuates spinal astrocytic activation in pain models[40] but can also enhance autophagy and ER stress via IRE1-TRAF2-ASK1-JNK signaling[41]. Collectively, these findings highlight that ketamine exerts nuanced and bidirectional regulation of MAPK signaling, with outcomes determined by tissue type, brain region, and dose.

The results of the open field and Barnes maze tests indicate that ketamine induces hyperlocomotion and impairs spatial learning and memory in mice, effects that are significantly attenuated by JNK inhibition, supporting an association between JNK signaling and ketamine-induced hyperactivity and cognitive impairment. Studies by Inoue et al. [42] and Sherrin et al. [43], employing C. elegans and mouse models, demonstrated that JNK deficiency enhances memory. Moreover, a 2018 study[44] reported that mice with JIP1-mediated impairment of JNK activation displayed enhanced performance in hippocampus-dependent tasks, including contextual fear conditioning and the Morris water maze. Collectively, these findings support the concept that JNK signaling acts as a negative regulator of learning and memory, consistent with our observation that JNK inhibition attenuates ketamine-induced cognitive deficits in mice. Beyond cognitive effects, additional studies[45] have shown that systemic administration of JNK antagonists reduces exploratory

ARTICLE IN PRESS

behavior in the open field in both acute stress–exposed and healthy mice, indicating that JNK also modulates anxiety-related and locomotor behaviors. Taken together, these results suggest that JNK plays a multifaceted role in the central nervous system, integrating regulatory effects on learning, memory, and general behavioral responses.

Our research findings present several phenomena that merit detailed discussion. Notably, an increase in H3S10ph was observed in HT22 hippocampal neuron cells of mice exposed to high doses of ketamine, whereas this phosphorylation elevation was not detected in the PFC and hippocampus. Although direct evidence elucidating the cause of this discrepancy remains elusive, the previous studies provide indirect evidence that may explain this phenomenon [46]. The H3S10ph reached its peak at one hour after treatment and returned to baseline within three hours post-induction. In our study, the behavioral tests after ketamine administration may inadvertently overlook the peak phosphorylation period, resulting in observations of phosphorylation levels reverting to baseline. Consequently, we excluded the behavioral experiments prior to RNA-seq and conducted protein detection 30 minutes after injection on Day 7 and we observed an elevation in H3S10ph.

Additionally, we observed a reduction in ERK phosphorylation levels in HT22 cells following ketamine treatment, while ERK phosphorylation levels were elevated in the PFC and hippocampus of mice following ketamine injection. Previous research has confirmed the elevation in ERK phosphorylation within the nucleus accumbens in rats after ketamine administration. Ketamine may

ARTICLE IN PRESS

induce DRD1 activation, thereby augmenting ERK phosphorylation [39]. Yet another investigation showed that DRD1 antagonists increased hippocampal ERK phosphorylation in morphine-addicted rats[47]. This discrepancy may be ascribed to ketamine's differential regulation of ERK phosphorylation across various cell types and brain regions, reflecting its multifaceted neurophysiological effects.

H3S10ph is a rapid, stimulus-coupled nucleosomal mark that facilitates chromatin remodeling and immediate-early gene transcription[48–50]. To determine whether ketamine-induced JNK–H3S10ph activation is accompanied by corresponding epigenomic and transcriptional changes, we performed paired ATAC-seq and RNA-seq at the established peak of H3S10ph elevation (30 minutes post-ketamine). At the transcriptome level, enrichment of MAPK signaling and serine/threonine kinase activator activity among DEGs, together with MAP3K9 emerging as a network hub, provides independent transcriptome-level support for JNK pathway activation, corroborating the protein-level findings reported above.

At the chromatin level, the predominant localization of DARs to distal intergenic regions rather than gene promoters, combined with enrichment of CTCF and CTCFL motifs in promoter-proximal DARs, suggests that ketamine-induced chromatin remodeling preferentially reorganizes three-dimensional chromatin architecture via CTCF-mediated enhancer–promoter looping rather than directly opening gene promoters[51]. The limited DAR–DEG overlap at 30 minutes is consistent with a temporal hierarchy in which enhancer

ARTICLE IN PRESS

accessibility precedes steady-state transcriptional changes[52], and supports an enhancer-priming interpretation rather than a disconnect between chromatin and transcriptional responses. The co-identification of SP9 and ACE2 at both the chromatin accessibility and transcriptional levels nominates them as candidate factors bridging early epigenetic remodeling to downstream gene expression, though their functional roles require direct experimental validation. Collectively, these multi-omics findings are consistent with a model in which JNK-mediated H3S10ph preferentially remodels distal regulatory elements to prime transcriptional programs, with full transcriptional consequences likely extending beyond the 30-minute window examined here. Direct causality between H3S10ph, chromatin remodeling, and behavioral outcomes remains to be established; targeted ChIP-seq for H3S10ph, time-course ATAC-seq, and cell-type-resolved single-cell approaches are warranted to address this.

To explore upstream regulation, we examined EXM1-Cre$^{+/-}$;DRD1^flox/flox mice with cortical excitatory neuron-specific DRD1 deletion. DRD1 knockout increased basal p-H3S10ph in both hippocampus and PFC, yet did not consistently alter JNK activation, and ketamine-induced H3S10ph persisted in cKO mice. These results indicate that DRD1 may modulate baseline phosphorylation levels but does not directly mediate ketamine-induced JNK–H3S10ph signaling, suggesting a modulatory rather than causal upstream role. Notably, ketamine produced opposing behavioral and molecular effects in cKO mice relative to NC controls, including improved spatial learning and

ARTICLE IN PRESS

attenuated H3S10ph, suggesting that the behavioral consequences of ketamine are sensitive to the integrity of DRD1-dependent dopaminergic signaling. This contrasting phenotype may reflect compensatory shifts in circuit-level responses following DRD1 deletion, potentially involving altered balance between dopaminergic and glutamatergic transmission[53], though the precise mechanistic basis remains to be established. Interestingly, trends in p-P38 parallel H3S10ph changes, suggesting a potential modulatory role for other MAPK branches that warrants further investigation.

There are still several limitations. Initially, despite the utilization of blood samples from individuals with schizophrenia, in vitro cell models, and animal models, each approach possesses inherent limitations. For instance, HT22 cell lines and C57 mouse models may not accurately replicate the complexity of human schizophrenia. Particularly for behavioral phenotypes involving extensive neural network and environmental interactions, the applicability of these models is constrained. In behavioral tests, ketamine-induced models exhibited increased locomotor activity and impaired learning and memory, but these reflect psychotic-like behavioral alterations rather than a disease state. Therefore, the repeated ketamine administration paradigm is widely used to model schizophrenia-related psychotic-like behaviors, but it does not constitute a disease model of schizophrenia itself. In addition, although JNK inhibition alleviated ketamine-induced behavioral and molecular alterations, the absence of complementary JNK activation experiments limits our ability to establish causality and pathway sufficiency. Moreover, additional

ARTICLE IN PRESS

pharmacological modulators used in vitro were not evaluated in vivo, which may have provided further resolution for distinguishing pathway-specific contributions to ketamine-induced behavioral phenotypes. Through transcriptome sequencing and chromatin open reading frame sequencing, the purpose of this study was to reveal the changes of gene expression caused by ketamine. However, it is not entirely clear whether these changes directly lead to the behavior of schizophrenia, or whether there are other intermediary mechanisms. The mechanism needs to be further revealed in the future. The present multi-omics analyses are mainly correlative and lack cell-type and temporal resolution to define precise regulatory mechanisms. Future studies using single-cell and time-resolved approaches are needed to further clarify the downstream network underlying ketamine-induced effects.

5. Conclusion

In conclusion, this study demonstrates that ketamine preferentially activates the JNK signaling pathway, leading to rapid phosphorylation of histone H3 at Ser10 in neuronal cells and in the mouse hippocampus. Pharmacological inhibition of JNK effectively attenuated ketamine-induced hyperlocomotion and cognitive impairment, supporting a functional contribution of JNK-dependent chromatin modification to psychotic-like behavioral alterations. Early hippocampal multi-omics profiling further revealed coordinated changes in gene expression and chromatin accessibility, particularly at distal regulatory elements enriched for MAPK signaling, neuroactive ligand–receptor interactions, and synaptic function, with CTCF emerging as a

ARTICLE IN PRESS

potential regulatory factor. Although causality between H3S10ph, chromatin remodeling, and transcriptional outcomes requires further validation, our findings establish JNK-mediated histone phosphorylation as a mechanistic link between intracellular signaling responses and ketamine-induced molecular and behavioral phenotypes. Together, this work provides an integrated epigenetic framework for understanding ketamine ' s neuropsychiatric effects and highlights JNK-H3S10ph signaling as a promising target for future mechanistic and therapeutic investigations in psychotic-like behavioral alterations.

Funding

The study was supported by Department of Science and Technology of Liaoning province (2024JH2/101900012).

ARTICLE IN PRESS

Ethics statement

The experimental protocol was approved by the Ethics Committee for Animal Experiments of China Medical University.

Author Contributions

Xiu-mei Zhu – Investigation, Data curation, Writing – original draft. Yang Li – Formal analysis, Visualization. Wenrui Liu – Methodology, Validation. Ying Pan – Investigation, Resources. Ang Li – Investigation, Validation. Gui-na Han – Formal analysis, Visualization. Hongbo Wang - Conceptualization,

ARTICLE IN PRESS

Funding acquisition, Supervision. Jun Yao – Conceptualization, Supervision, Writing – review & editing.

Competing interests

The authors declare that they have no competing interests.

Consent for publication

Not applicable.

Availability of data and materials

The datasets used or analyzed during the current study are available from the corresponding author upon reasonable request.

ARTICLE IN PRESS

References

1. Curran, H. V. & Morgan, C. Cognitive, dissociative and psychotogenic effects of ketamine in recreational users on the night of drug use and 3 days later. *Addict. Abingdon Engl.* **95**, 575–590 (2000).
2. Hirota, K. & Lambert, D. G. Ketamine; history and role in anesthetic pharmacology. *Neuropharmacology* **216**, 109171 (2022).
3. Le Daré, B., Pelletier, R., Morel, I. & Gicquel, T. Histoire de la kétamine : une molécule ancienne qui a toujours la cote. *Ann. Pharm. Fr.* **80**, 1–8 (2022).
4. NMDA receptor antagonist effects, cortical glutamatergic function, and schizophrenia: toward a paradigm shift in medication development | Psychopharmacology. https://link.springer.com/article/10.1007/s00213-003-1582-z.
5. Chatterjee, M., Verma, R., Ganguly, S. & Palit, G. Neurochemical and molecular characterization of ketamine-induced experimental psychosis model in mice. *Neuropharmacology* **63**, 1161–1171 (2012).
6. Steeds H., Carhart-Harris R. L. & Stone J. M. Drug models of schizophrenia. *Ther. Adv. Psychopharmacol.* **5**, 43 (2015).
7. Sub-Chronic Ketamine Administration Increases Dopamine Synthesis Capacity in the Mouse Midbrain: a Preclinical In Vivo PET Study | Molecular Imaging and Biology. https://link.springer.com/article/10.1007/s11307-023-01865-y.
8. Deng, L. *et al.* Dynamic aberrances of substantia nigra-relevant coactivation patterns in first-episode treatment-naïve patients with schizophrenia. *Psychol. Med.* 1–11 (2024) doi:10.1017/S0033291724000655.
9. Different projection neurons of basolateral amygdala participate in the retrieval of morphine withdrawal memory with diverse molecular pathways | Molecular Psychiatry. https://www.nature.com/articles/s41380-023-02371-x.

ARTICLE IN PRESS

10. Funk, A. J., McCullumsmith, R. E., Haroutunian, V. & Meador-Woodruff, J. H. Abnormal activity of the MAPK- and cAMP-associated signaling pathways in frontal cortical areas in postmortem brain in schizophrenia. *Neuropsychopharmacol. Off. Publ. Am. Coll. Neuropsychopharmacol.* **37**, 896–905 (2012).
11. Xu, Z., Wen, C. & Wang, W. Role of MAPK and PI3K-Akt signaling pathways in cuprizone-induced demyelination and cognitive impairment in mice. *Behav. Brain Res.* **458**, 114755 (2024).
12. Deane, A. R., Potemkin, N. & Ward, R. D. Mitogen-activated protein kinase (MAPK) signalling corresponds with distinct behavioural profiles in a rat model of maternal immune activation. *Behav. Brain Res.* **396**, 112876 (2021).
13. Brami-Cherrier, K., Lavaur, J., Pagès, C., Arthur, J. S. C. & Caboche, J. Glutamate induces histone H3 phosphorylation but not acetylation in striatal neurons: role of mitogen- and stress-activated kinase-1. *J. Neurochem.* **101**, 697–708 (2007).
14. Lee, Y. J. & Shukla, S. D. Histone H3 phosphorylation at serine 10 and serine 28 is mediated by p38 MAPK in rat hepatocytes exposed to ethanol and acetaldehyde. *Eur. J. Pharmacol.* **573**, 29–38 (2007).
15. Browning, J. L. *et al.* Clozapine and the mitogen-activated protein kinase signal transduction pathway: implications for antipsychotic actions. *Biol. Psychiatry* **57**, 617–623 (2005).
16. Tiwari, V. K. *et al.* A chromatin-modifying function of JNK during stem cell differentiation. *Nat. Genet.* **44**, 94–100 (2011).
17. Brami-Cherrier, K., Roze, E., Girault, J.-A., Betuing, S. & Caboche, J. Role of the ERK/MSK1 signalling pathway in chromatin remodelling and brain responses to drugs of abuse. *J. Neurochem.* **108**, 1323–1335 (2009).
18. Chwang, W. B., O'Riordan, K. J., Levenson, J. M. & Sweatt, J. D. ERK/MAPK regulates hippocampal histone phosphorylation following contextual fear conditioning. *Learn. Mem. Cold Spring Harb. N* **13**, 322–328 (2006).
19. Shi, M. *et al.* Effects of Ketamine on Learning and Memory in the Hippocampus of Rats through ERK, CREB, and Arc. *Brain Sci.* **11**, 27 (2020).
20. Huang, L., Liu, Y., Jin, W., Ji, X. & Dong, Z. Ketamine potentiates hippocampal neurodegeneration and persistent learning and memory impairment through the PKCγ–ERK signaling pathway in the developing brain. *Brain Res.* **1476**, 164–171 (2012).
21. Sharma, R. P., Feiner, B. & Chase, K. A. Histone H3 phosphorylation is upregulated in PBMCs of schizophrenia patients in comparison to healthy controls. *Schizophr. Res.* **169**, 498–499 (2015).
22. Li, X.-J. *et al.* Ketamine enhances dopamine D1 receptor expression by modulating microRNAs in a ketamine-induced schizophrenia-like mouse model. *Neurotoxicol. Teratol.* **91**, 107079 (2022).
23. Gorski, J. A. *et al.* Cortical Excitatory Neurons and Glia, But Not GABAergic Neurons, Are Produced in the Emx1-Expressing Lineage. *J. Neurosci.* **22**, 6309–6314 (2002).
24. Zhang, Q., Huang, Y., Zhang, L., Ding, Y.-Q. & Song, N.-N. Loss of Satb2 in the Cortex and Hippocampus Leads to Abnormal Behaviors in Mice. *Front. Mol. Neurosci.* **12**, (2019).
25. Guo, H. *et al.* Specificity and efficiency of Cre-mediated recombination in Emx1-Cre knock-in mice. *Biochem. Biophys. Res. Commun.* **273**, 661–665 (2000).
26. Neuronal injury, but not microglia activation, is associated with ketamine-induced experimental schizophrenic model in mice. *Prog. Neuropsychopharmacol. Biol. Psychiatry* **45**, 107–116 (2013).
27. Imami, A. *et al.* Perturbation of Cell-subtype specific Active Kinome Networks in Schizophrenia. https://doi.org/10.5281/zenodo.17334341 doi:10.5281/zenodo.17334341.
28. Igolkina, A. A. *et al.* Analysis of Gene Expression Variance in Schizophrenia Using Structural Equation Modeling. *Front. Mol. Neurosci.* **11**, 192 (2018).
29. Malik, J. A. *et al.* Understanding translational research in schizophrenia: A novel insight into animal models. *Mol. Biol. Rep.* **50**, 3767–3785 (2023).

ARTICLE IN PRESS

30. Hess, J. L. *et al.* Transcriptome-Wide Mega-Analyses Reveal Joint Dysregulation of Immunologic Genes and Transcription Regulators in Brain and Blood in Schizophrenia. *Schizophr. Res.* **176**, 114–124 (2016).
31. Formaldehyde-induced histone H3 phosphorylation via JNK and the expression of proto-oncogenes. *Mutat. Res. Mol. Mech. Mutagen.* **770**, 9–18 (2014).
32. Cigarette sidestream smoke induces histone H3 phosphorylation via JNK and PI3K/Akt pathways, leading to the expression of proto-oncogenes | Carcinogenesis | Oxford Academic. https://academic.oup.com/carcin/article-abstract/35/6/1228/449461.
33. Coordinated regulation of Nrf2 and histone H3 serine 10 phosphorylation in arsenite-activated transcription of the human heme oxygenase-1 gene. *Biochim. Biophys. Acta BBA - Gene Regul. Mech.* **1849**, 1277–1288 (2015).
34. Lee, K. & Song, K. Basal c-Jun N-terminal kinases promote mitotic progression through histone H3 phosphorylation. *Cell Cycle* **7**, 216–221 (2008).
35. Wu, G.-H. *et al.* Ketamine exerts dual effects on the apoptosis of primary cultured hippocampal neurons from fetal rats in vitro. *Metab. Brain Dis.* **38**, 2417–2426 (2023).
36. Ketamine reduces the induced spinal p38 MAPK and pro-inflammatory cytokines in a neuropathic rats - PubMed. https://pubmed.ncbi.nlm.nih.gov/24567814/.
37. Xu, H.-J., Li, X.-P. & Han, L.-Y. Role and mechanism of esketamine in improving postoperative cognitive dysfunction in aged mice through the TLR4/MyD88/p38 MAPK pathway. *Kaohsiung J. Med. Sci.* **40**, 63–73 (2024).
38. Salort, G., Álvaro-Bartolomé, M. & García-Sevilla, J. A. Ketamine-induced hypnosis and neuroplasticity in mice is associated with disrupted p-MEK/p-ERK sequential activation and sustained upregulation of survival p-FADD in brain cortex: Involvement of GABAA receptor. *Prog. Neuropsychopharmacol. Biol. Psychiatry* **88**, 121–131 (2019).
39. Miao, H.-C., Liu, M., Wu, F. & Li, H.-B. Expression changes of c-Fos and D1R/p-ERK1/2 signal pathways in nucleus accumbens of rats after ketamine abuse. *Biochem. Biophys. Res. Commun.* **629**, 183–188 (2022).
40. Mei, X.-P. *et al.* Inhibition of spinal astrocytic c-Jun N-terminal kinase (JNK) activation correlates with the analgesic effects of ketamine in neuropathic pain. *J. Neuroinflammation* **8**, 6 (2011).
41. Yu, Y., Wu, D., Li, Y., Qiao, H. & Shan, Z. Ketamine enhances autophagy and endoplasmic reticulum stress in rats and SV-HUC-1 cells via activating IRE1-TRAF2-ASK1-JNK pathway. *Cell Cycle Georget. Tex* **20**, 1907–1922 (2021).
42. Inoue, A. *et al.* Forgetting in C. elegans is accelerated by neuronal communication via the TIR-1/JNK-1 pathway. *Cell Rep.* **3**, 808–819 (2013).
43. Sherrin, T. *et al.* Hippocampal c-Jun-N-Terminal Kinases Serve as Negative Regulators of Associative Learning. *J. Neurosci.* **30**, 13348–13361 (2010).
44. Morel, C. *et al.* JIP1-Mediated JNK Activation Negatively Regulates Synaptic Plasticity and Spatial Memory. *J. Neurosci.* **38**, 3708–3728 (2018).
45. Clarke M., Pentz R., Bobyn J. & Hayley S. Stressor-Like Effects of c-Jun N-Terminal Kinase (JNK) Inhibition. *PLOS ONE* **7**, e44073 (2012).
46. Crosio, C., Heitz, E., Allis, C. D., Borrelli, E. & Sassone-Corsi, P. Chromatin remodeling and neuronal response: multiple signaling pathways induce specific histone H3 modifications and early gene expression in hippocampal neurons. *J. Cell Sci.* **116**, 4905–4914 (2003).
47. Mozafari, R. *et al.* Hippocampal D1—but not D2—like dopamine receptors modulate the phosphorylation of ERK in food deprivation-induced reinstatement of morphine in extinguished rats. *NeuroReport* **32**, 332 (2021).
48. Thomson, S. *et al.* The nucleosomal response associated with immediate-early gene induction is mediated via alternative MAP kinase cascades: MSK1 as a potential histone H3/HMG-14 kinase. *EMBO J.* **18**, 4779–4793 (1999).
49. Drobic, B., Pérez-Cadahía, B., Yu, J., Kung, S. K.-P. & Davie, J. R. Promoter chromatin remodeling of immediate-early genes is mediated through H3 phosphorylation at either

ARTICLE IN PRESS

ARTICLE IN PRESS

serine 28 or 10 by the MSK1 multi-protein complex. *Nucleic Acids Res.* **38**, 3196–3208 (2010).
50. Komar, D. & Juszczynski, P. Rebelled epigenome: histone H3S10 phosphorylation and H3S10 kinases in cancer biology and therapy. *Clin. Epigenetics* **12**, 147 (2020).
51. Yan, F., Powell, D. R., Curtis, D. J. & Wong, N. C. From reads to insight: a hitchhiker's guide to ATAC-seq data analysis. *Genome Biol.* **21**, 22 (2020).
52. Maytum, A. *et al.* Chromatin priming elements direct tissue-specific gene activity before hematopoietic specification. *Life Sci. Alliance* **7**, e202302363 (2023).
53. Yin, Y. *et al.* Astrocytic dopamine D1 receptor modulates glutamatergic transmission and synaptic plasticity in the prefrontal cortex through d-serine. *Acta Pharm. Sin. B* **15**, 4692–4710 (2025).

Table 1. HT22 cells treatment and grouping.

Group	1	2	3	4	5	6	7	8	9	10	11	12	13	14	15
Saline	+	+	+	+	+	+	+	+	+	+	+	+	+	+	+
Ketamine (10 μmol/L)	-	+	-	-	-	-	-	-	-	-	-	-	-	-	-
Ketamine (20 μmol/L)	-	-	+	-	-	-	-	-	-	-	-	-	-	-	-
Ketamine (50 μmol/L)	-	-	-	+	-	-	-	-	-	-	-	-	-	-	-
Ketamine (100 μmol/L)	-	-	-	-	+	-	-	-	-	-	-	-	-	-	-
Ketamine (200 μmol/L)	-	-	-	-	-	+	-	-	-	-	-	+	+	+	-
Ketamine (500 μmol/L)	-	-	-	-	-	-	+	-	-	-	-	-	-	-	-
Ketamine (1000 μmol/L)	-	-	-	-	-	-	-	+	-	-	-	-	-	-	-
P38 pathway inhibitor SB203580 (20 μmol/L)	-	-	-	-	-	-	-	-	+	-	-	+	-	-	-
ERK pathway inhibitor PD98059 (20 μmol/L)	-	-	-	-	-	-	-	-	-	+	-	-	-	-	-
JNK pathway inhibitor SP600125 (20 μmol/L)	-	-	-	-	-	-	-	-	-	-	+	-	+	-	-
P-ERK1/2 agonist Ro67-7476 (1 μmol/L)	-	-	-	-	-	-	-	-	-	-	-	-	-	+	+

ARTICLE IN PRESS

ARTICLE IN PRESS

Table 2. The list of bioactive molecules used in cells and mice.

Bioactive molecule	Cat. #	Company	Concentration
P38 pathway inhibitor SB203580	HY-10256	MCE	20 μmol/L for cells
ERK pathway inhibitor PD98059	HY-12028	MCE	20 μmol/L for cells
P-ERK1/2 agonist Ro67-7476	HY-100403	MCE	1 μmol/L for cells
JNK pathway inhibitor SP600125	HY-12041	MCE	20 μmol/L for cells 15 mg/kg for mice

ARTICLE IN PRESS

ARTICLE IN PRESS

Table 3. Antibody list

Maker	Cat. #	Company	Dilution ratio	Host
Histone-H3	17168-1-AP	Proteintech	1:2000	rabbit
p-Ser10 Histone-H3	3377S	CST	1:1000 [1] 1:200 [2]	rabbit
JNK	sc-7345	Santa Cruz	1:500	mouse
p-JNK (Thr 183 and Tyr 185)	sc-6254	Santa Cruz	1:500	mouse
ERK	sc-514302	Santa Cruz	1:500	mouse
p-ERK (Tyr 204)	sc-7383	Santa Cruz	1:500	mouse
P38	sc-7972	Santa Cruz	1:500	mouse
p-P38 (t Tyr 182)	sc-7973	Santa Cruz	1:500	mouse
p-SEK1/MKK4 (Ser257)	#4514	CST	1:1000	rabbit
p-c-Jun (Ser63)	#2361	CST	1:1000	rabbit
p-ATF-2 (Thr71)/ATF-7 (Thr53)	#15411	CST	1:1000	rabbit
β-actin	TA-09	ZSGB-BIO	1:2000	mouse
β-Tubulin	TA-10	ZSGB-BIO	1:3000	mouse

1: Dilution ratio for western blot
2: Dilution ratio for immunofluorescence

ARTICLE IN PRESS

Figure 1. Protein levels of HT22 cells after treatments with eight different concentrations of ketamine and inhibitors/agonist for 24 hours

a. Classification and annotation of environmental information process pathways generated by comparing differentially expressed genes (DEGs) of patients with schizophrenia via KEGG database. b. Timeline of HT22 cells exposed to different concentrations of ketamine ranged from 0μmol/L to 1000μmol/L. c-d. Protein levels of p-JNK, JNK, p-ERK, ERK, p-P38, P38, p-H3 (Ser10) and Histone H3 of HT22 cells (n = 5). Western blot data were normalized to the NC group (0 μmol/L ketamine), and statistical comparisons were performed using one-sample t-test against the theoretical normalized value of 1. e. Timeline of ketamine and inhibitors/agonist treatments. f-g. P-H3 (Ser10), Histone H3, p-P38 and P38 protein levels of HT22 cells after the treatment of saline,

ARTICLE IN PRESS

200μmol/L ketamine, 20μmol/L P38 pathway inhibitor SB203580+200μmol/L ketamine and 20μmol/L SB203580 (n = 4). h-i. P-H3 (Ser10), Histone H3, p-ERK and ERK protein levels of HT22 cells under the treatment of saline, 200μmol/L ketamine, 1μmol/L p-ERK1/2 agonist Ro-67-7476+200μmol/L ketamine and 1μmol/L Ro-67-7476 (n = 3). j-k. P-H3 (Ser10), Histone H3, p-JNK and JNK protein levels of HT22 cells under the treatment of saline, 200μmol/L ketamine, 20μmol/L JNK pathway inhibitor SP600125+200μmol/L and 20μmol/L SP600125 (n = 4). Western blot data in f-k were normalized to the NC (saline) group, and statistical comparisons were performed using two-way ANOVA followed by Sidak's multiple comparisons test. Data were presented as the mean ± standard deviation. The significance of differences compared to the NC group data was indicated by "*" (*$p < 0.05$, **$p < 0.01$, ***$p < 0.001$) and the significance of differences compared to the KET group data was indicated by "#" (#$p < 0.05$, ##$p < 0.01$, ###$p < 0.001$).

ARTICLE IN PRESS

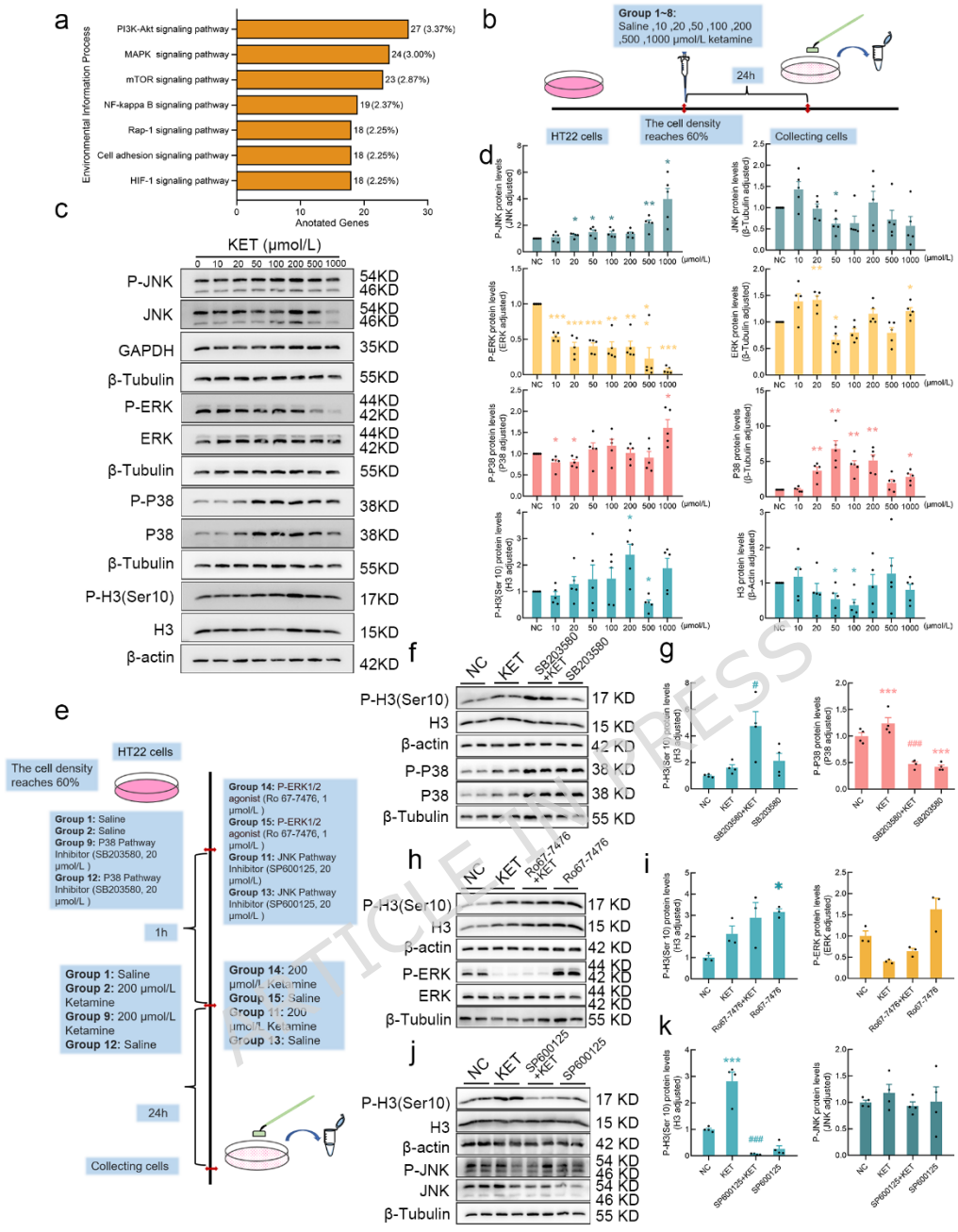


Figure 2. Immunofluorescence analysis of p-H3 (Ser10) in HT22 cells

a-b. Immunofluorescence of p-H3 (Ser10) of HT22 cells after treatments with saline, 200μmol/L ketamine, 20μmol/L SB203580+200μmol/L ketamine, 20μmol/L SB203580, 1μmol/L Ro67-7476+ketamine, 1μmol/L Ro67-7476, 20μmol/L SP600125+ketamine and 20μmol/L SP600125 for 24 hours (n = 12 independent samples per group). Data were presented as the mean ± standard deviation. Statistical comparisons among the eight

ARTICLE IN PRESS

groups were performed using one-way ANOVA followed by Tukey's multiple comparisons test. The significance of differences compared to the NC group data was indicated by "*" (*$p < 0.05$, **$p < 0.01$, ***$p < 0.001$) and the significance of differences compared to the KET group data was indicated by "#" (#$p < 0.05$, ##$p < 0.01$, ###$p < 0.001$).

ARTICLE IN PRESS

ARTICLE IN PRESS

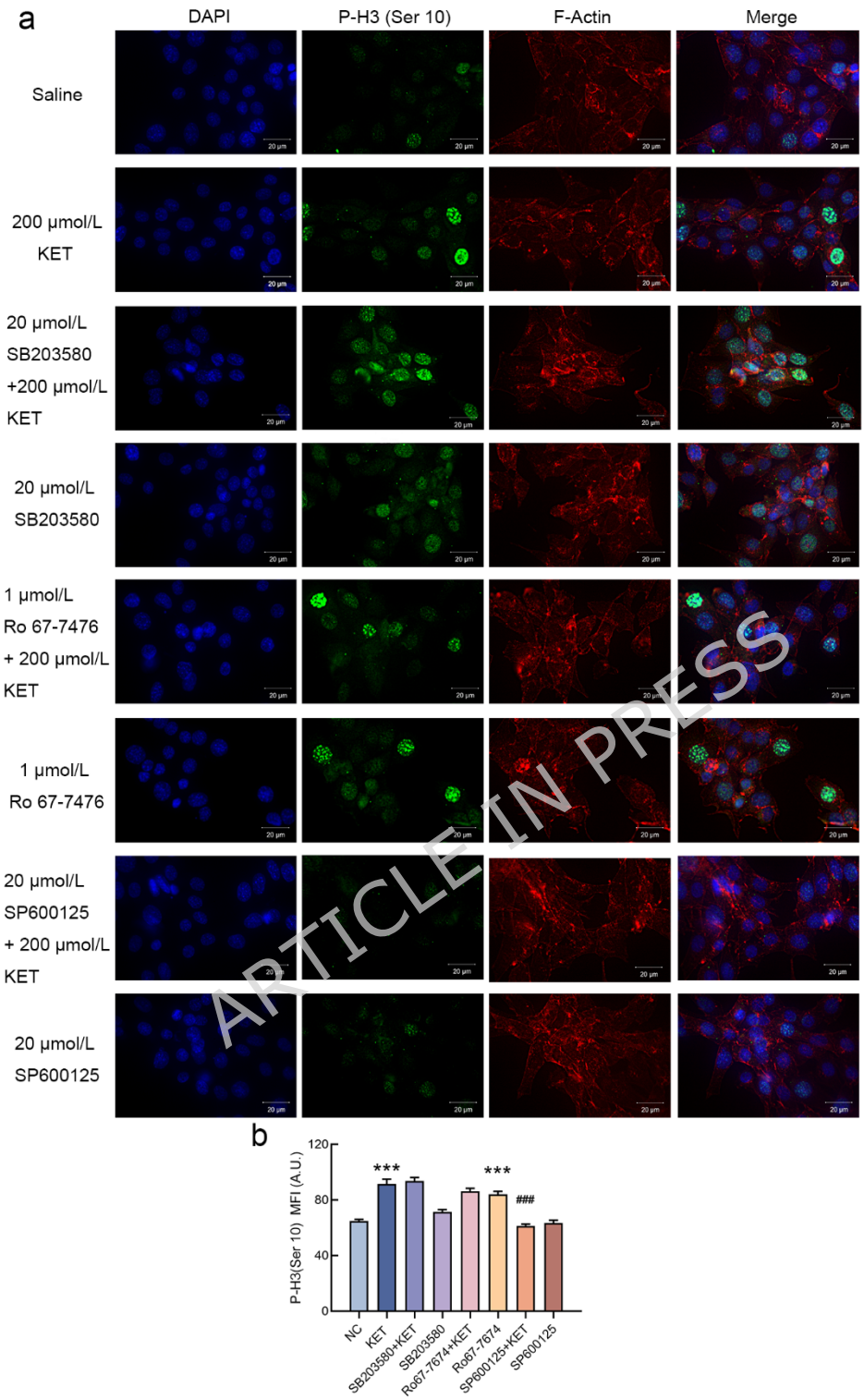


Figure 3. Behavioral tests and protein levels in the PFC and hippocampus of mice for the NC, KET, SP600125+KET and SP600125 groups

a. Timeline of intraperitoneal drug injection, behavioral tests and tissue collecting. b.

ARTICLE IN PRESS

Left: path diagrams for the open field tests of the four groups. Right: hot point map displaying the movement speed of mice from the four groups. c. Total distances, moving duration and central zone crossing times in the open field tests for the four groups (n = 6). Statistical analyses of the open field test data were performed using repeated-measures two-way ANOVA followed by Sidak's multiple comparisons test. d. Path diagrams for the Barnes maze tests of the four groups. e. Toal distances traveled, latency and number of error holes before the mice into the target hole in Barnes maze. Statistical analyses of the Barnes maze test data were performed using two-way ANOVA followed by Sidak's multiple comparisons test (n = 6). f-h. P-H3 (Ser10), H3, p-JNK, JNK, p-MKK4, p-ATF2 and p-c-Jun protein levels in the PFC and hippocampus of mice for the four groups (n = 6). Statistical analyses were performed using two-way ANOVA followed by Sidak's multiple comparisons test. i. P-H3 (Ser10) and H3 protein levels in the hippocampus from both the NC and KET groups of mice 30 mins post-injection (n = 3), and statistical comparisons were performed using unpaired (independent) two-tailed t-test. All western blot data were normalized to the NC group and data were presented as the mean ± standard deviation. The significance of differences compared to the NC group data was indicated by the symbol "*" (*p < 0.05, **p < 0.01, ***p < 0.001) and the significance of differences compared to the KET group data was indicated by the symbol "#" (#p < 0.05, ##p < 0.01, ###p < 0.001).

ARTICLE IN PRESS

ARTICLE IN PRESS

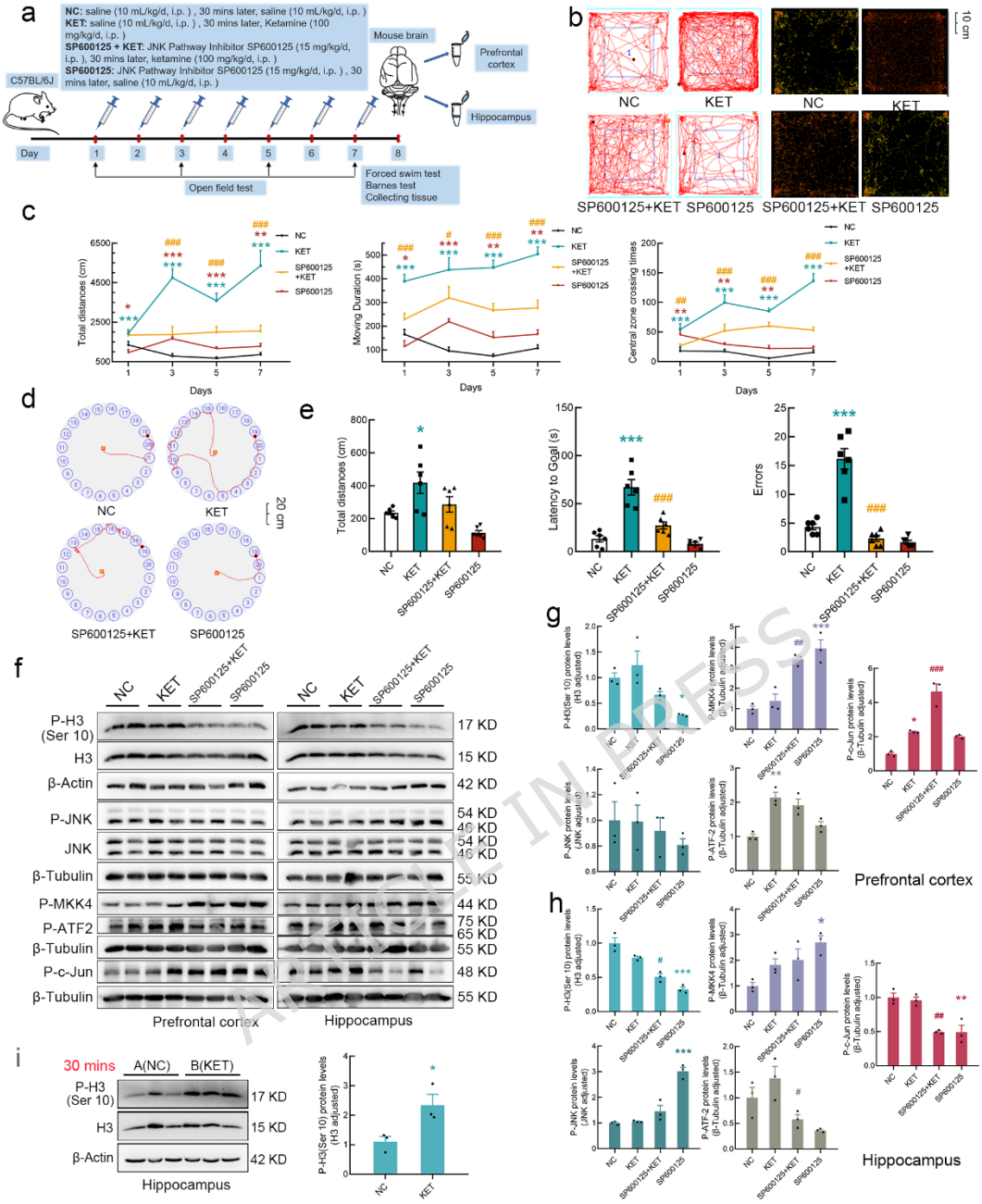


Figure 4. Analysis of RNA-seq of hippocampal tissue from NC and KET groups of mice (n = 4)

a. Timeline of intraperitoneal drug injection, tissue collecting, RNA-seq and ATAC-seq.

b. Left: the number of differentially expressed genes (DEGs) between NC group and KET group (A vs B) (selection criteria of DEGs: |Fold Change|≥1.5 and P value < 0.05) Right: DEGs volcano plot c. Hierarchical cluster analysis heat map of DEGs across all samples.

d. KEGG pathway classification map of DEGs

ARTICLE IN PRESS

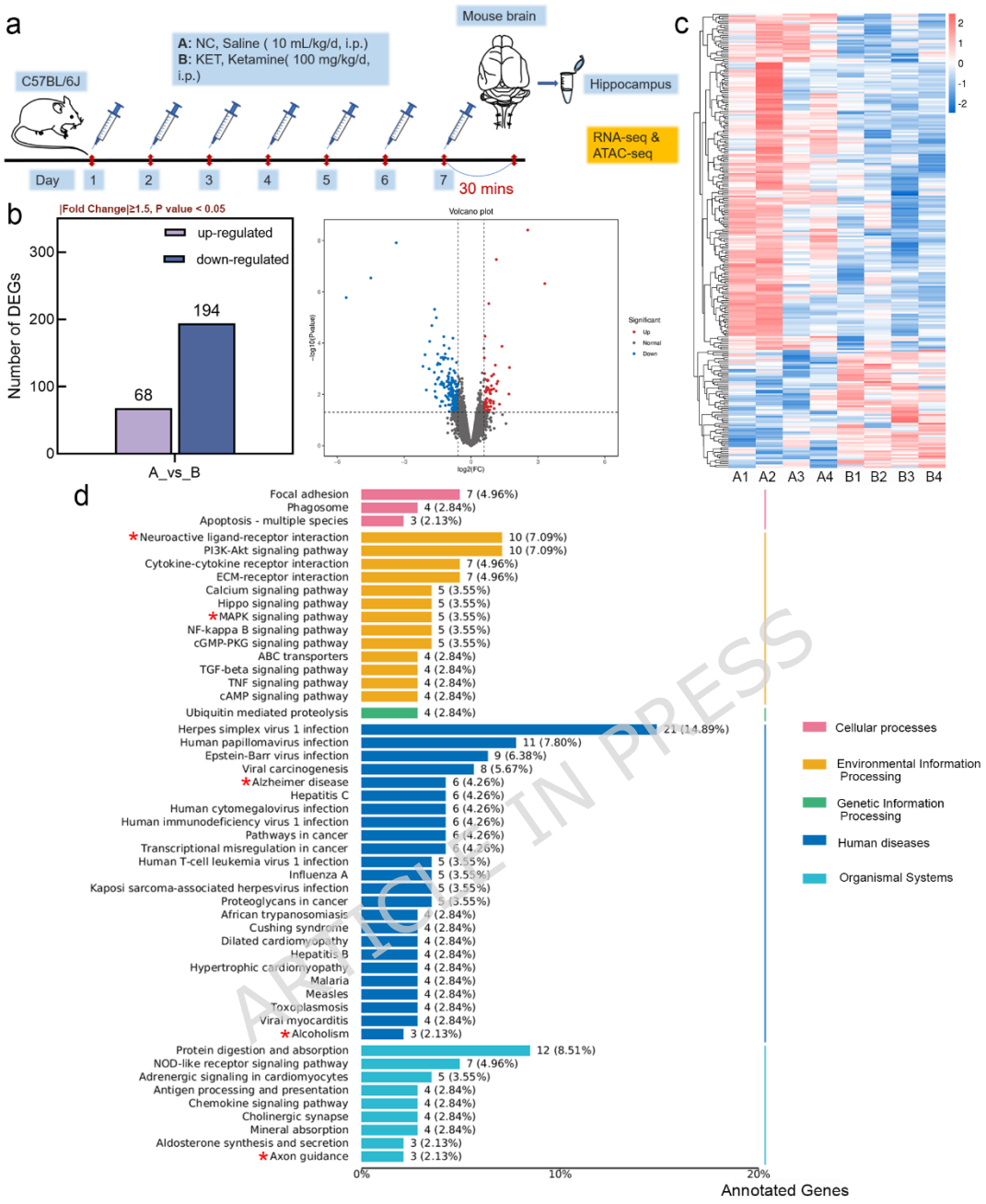


Figure 5. Analysis of ATAC-Seq of hippocampal tissue from NC and KET groups of mice a. Volcano plot of differentially accessible regions (DARs) between NC and KET groups (A vs B), with selection criteria: |Fold Change| ≥ 2, FDR < 0.05 b. Annotation classification plot of differentially accessible peak regions c. KEGG pathway enrichment scatter plot for genes associated with differential peaks in the promoter region d. GO enrichment plot for genes associated with differential peaks in the promoter region

(Molecular Function) e. Enrichment bubble plot comparing motifs from all samples to known transcription factors in the database. Significantly enriched motifs were identified using MEME-CHIP with a threshold of $P < 0.05$. f. Above: motif annotation of differential peaks below: annotated motifs and their associated target genes

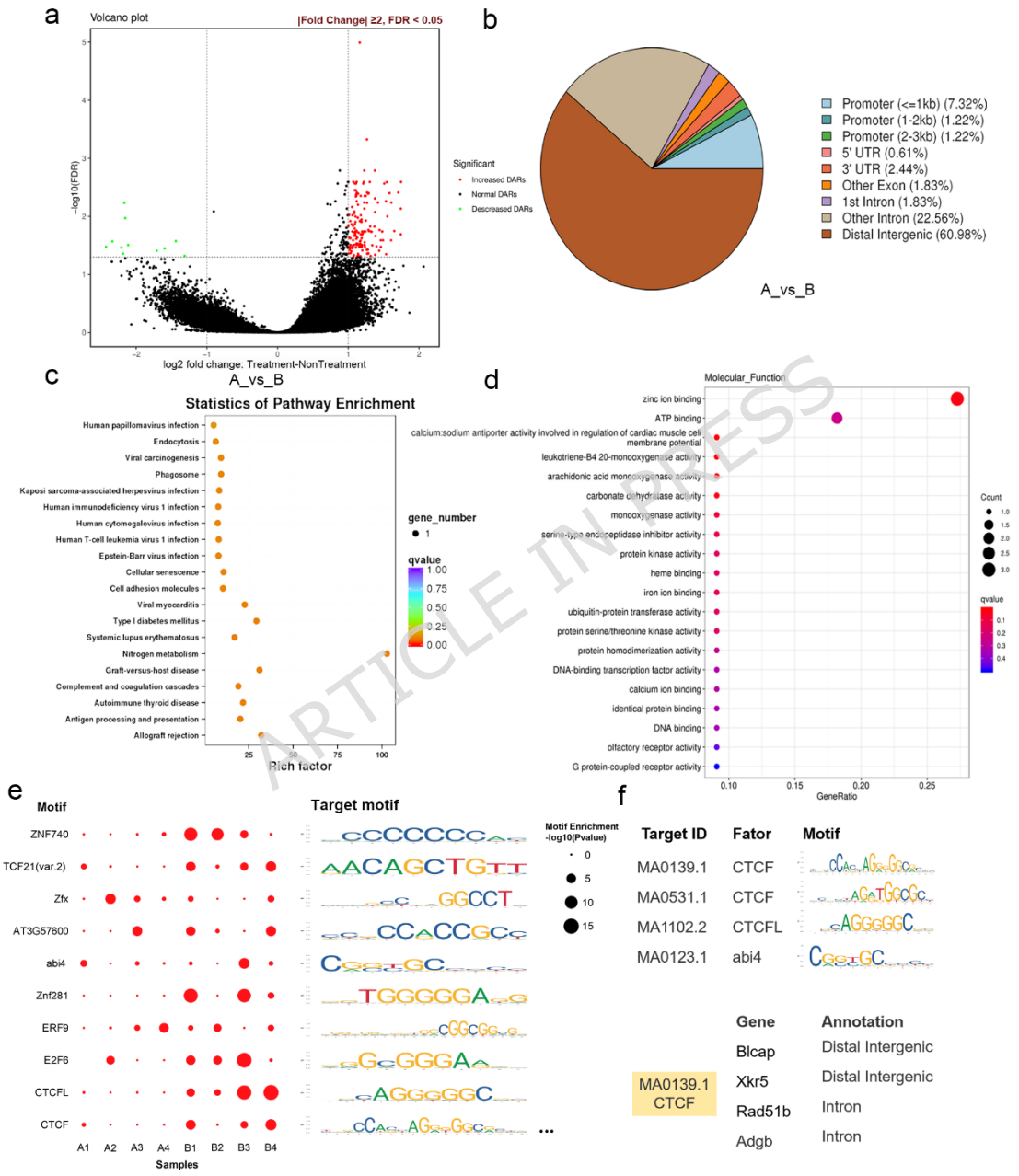


Figure S1. RNA-seq of peripherical blood of healthy individuals and patients with schizophrenia

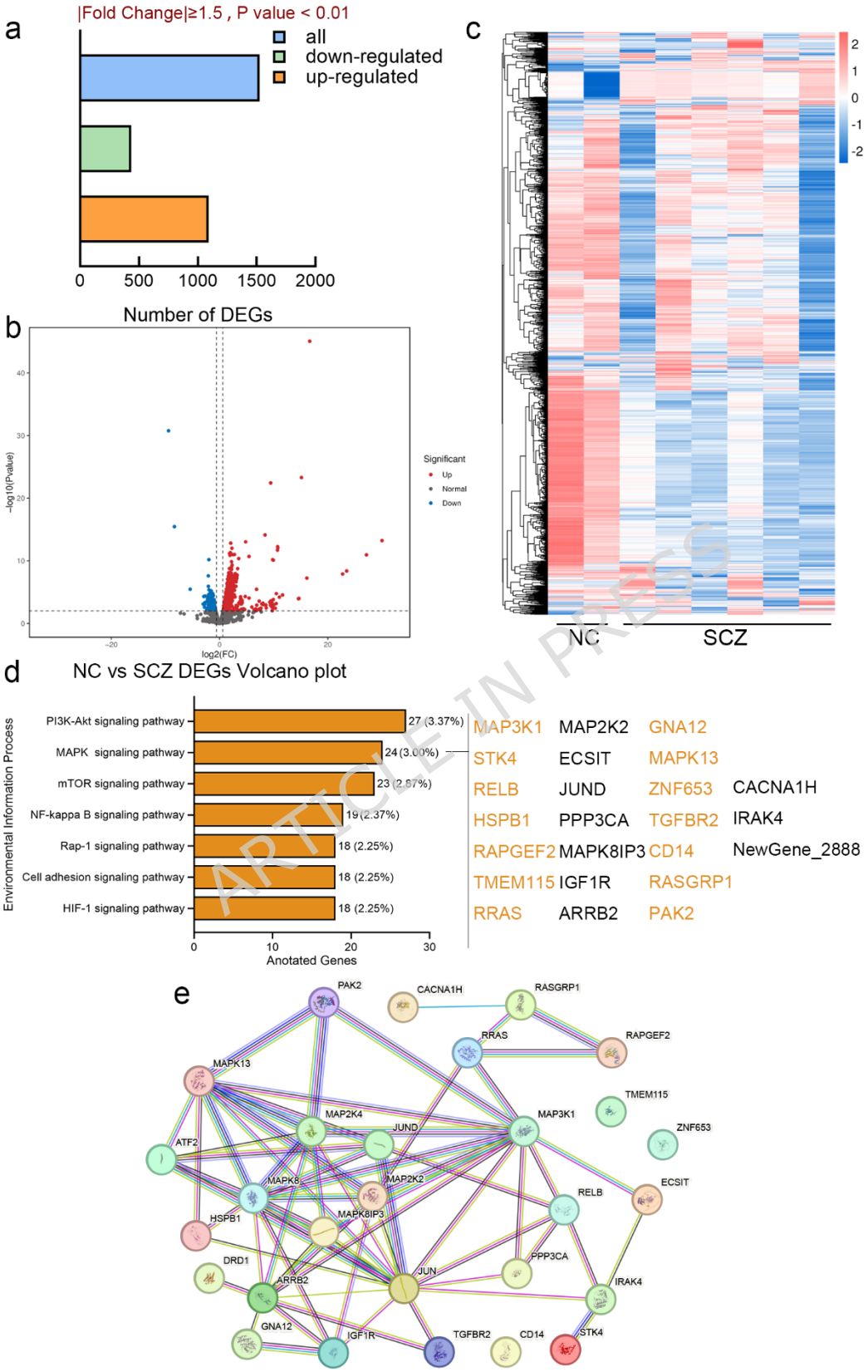
a. The number of DEGs between healthy individuals and patients with schizophrenia (NC

ARTICLE IN PRESS

vs SCZ, selection criteria of DEGs: |Fold Change|≥1.5 and P value < 0.01) b. Volcano map of differential expression between NC vs SCZ c. Hierarchical cluster analysis heat map of DEGs d. Classification and annotation of environmental information pathways based on DEGs comparison between NC and SCZ in the KEGG database e. Interaction network of MAPK pathway-related gene homologues proteins and related proteins

ARTICLE IN PRESS

ARTICLE IN PRESS



ARTICLE IN PRESS

Figure S2. The results of HT22 pre-experiment and other data of mouse behavioral tests a. Timeline of HT22 cells exposed to ketamine, SB203580, PD98059 and SP600125 treatments. b-c. Protein levels of p-JNK, JNK, p-ERK, ERK, p-P38, P38, p-H3 (Ser10) and Histone H3 of HT22 cells for saline, ketamine, SB203580, PD98059 and SP600125 groups (n = 4). Western blot data were normalized to the NC group, and statistical comparisons were performed using one-sample t-test against the theoretical normalized value of 1. d. Center zone moving duration percents and center zone moving distance percents in the open field tests of the mice for NC, KET, SP600125+KET and SP600125 groups e. Resting time in forced swim tests of the mice for NC, KET, SP600125+KET and SP600125 groups. f. Center zone moving distance percents of the mice for the NC, KET, cKO-NC and cKO-KET groups. Statistical analyses of the open field test data were performed using repeated-measures two-way ANOVA, while the Barnes maze and forced swim test data were analyzed using two-way ANOVA, both followed by Šídák's multiple comparisons test. Data were presented as the mean ± standard deviation. The significance of differences compared to the NC group data was indicated by the symbol "*" (*$p < 0.05$, **$p < 0.01$, ***$p < 0.001$) and the significance of differences compared to the KET group data was indicated by the symbol "#" (#$p < 0.05$, ##$p < 0.01$, ###$p < 0.001$).

ARTICLE IN PRESS

ARTICLE IN PRESS

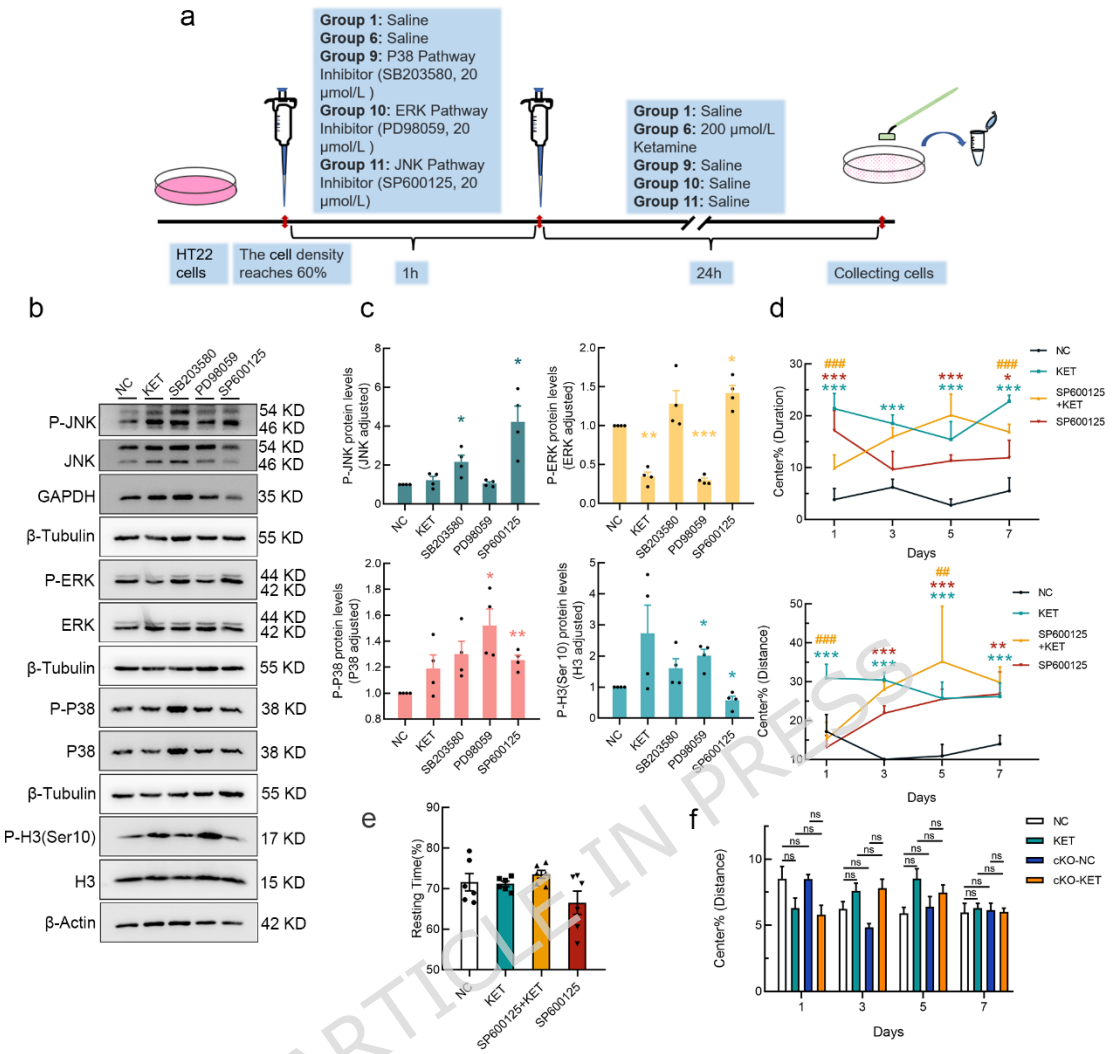


Figure S3. Behavioral tests and protein levels in the PFC and hippocampus of mice for the NC, KET, cKO-NC and cKO-KET groups

a. Timeline of intraperitoneal drug injection, behavioral tests and tissue collecting. b. Left: path diagrams for the open field tests of the four groups. Right: hot point map displaying the movement speed of mice from the four groups. c. Total distances, moving duration center zone moving duration percentage and central zone crossing times in the open field tests for the four groups (n= 5). Statistical analyses of the open field test data were performed using repeated-measures two-way ANOVA followed by Sidak's multiple comparisons test. d. Path diagrams for the Barnes maze tests of the four groups. e. Toal distances traveled and latency before the mice into the target hole in Barnes maze (n=

ARTICLE IN PRESS

5). f. The resting time in the forced swim tests of the four groups (n= 5). Statistical analyses of the Barnes maze and forced swim test data were performed using two-way ANOVA followed by Sidak's multiple comparisons test. g-i. p-JNK, JNK, p-MKK4, p-ATF2, p-c-Jun, p-ERK, ERK, p-P38, P38, P-H3 (Ser10) and H3 protein levels in the PFC and hippocampus of mice for the four groups (n= 3). Statistical analyses were performed using two-way ANOVA followed by Sidak's multiple comparisons test. Data were presented as the mean ± standard deviation. The significance of differences compared to the NC group data was indicated by the symbol "*" (*p < 0.05, **p < 0.01, ***p < 0.001) and the significance of differences compared to the KET group data was indicated by the symbol "#" (#p < 0.05, ##p < 0.01, ###p < 0.001).

ARTICLE IN PRESS

ARTICLE IN PRESS

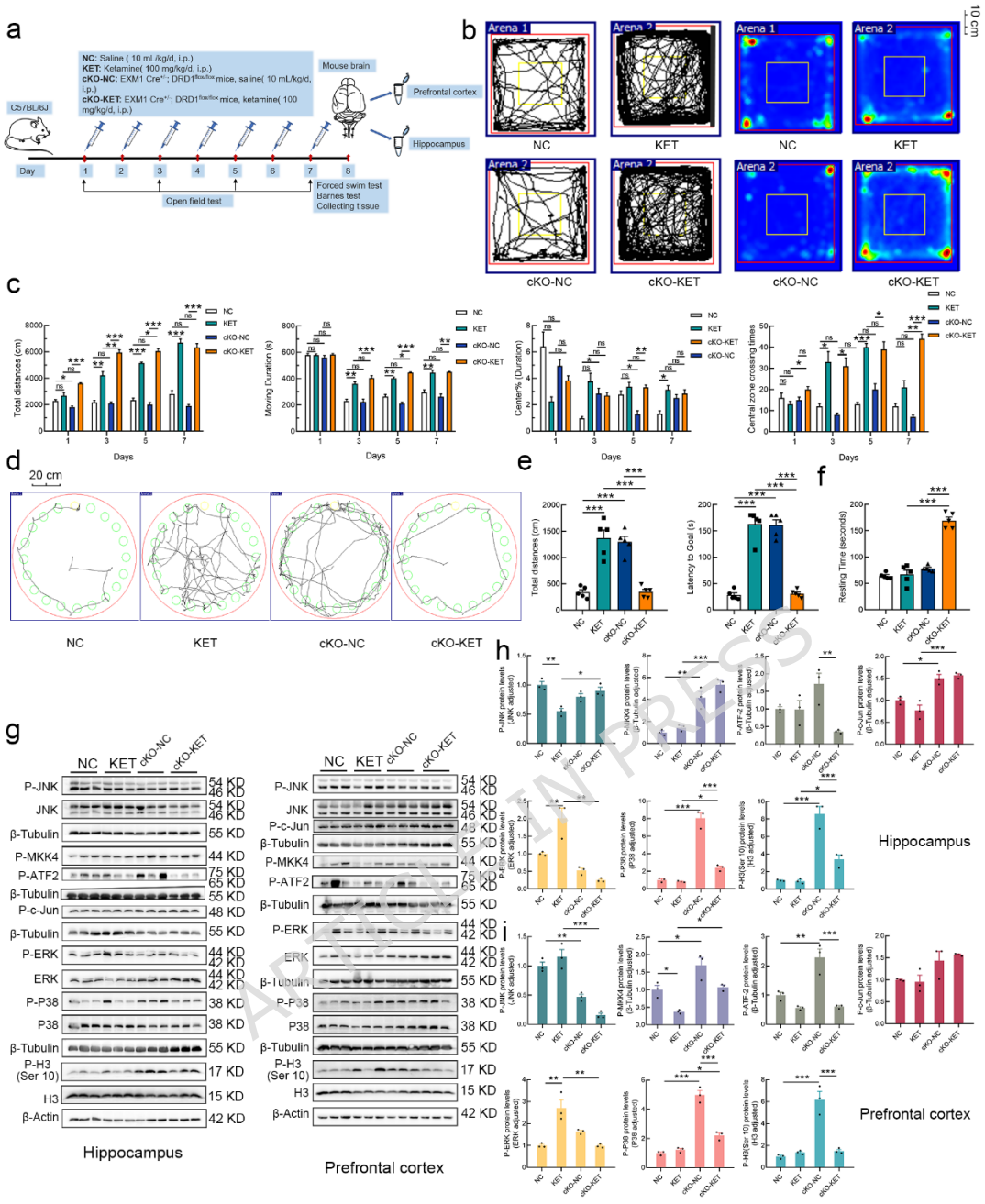
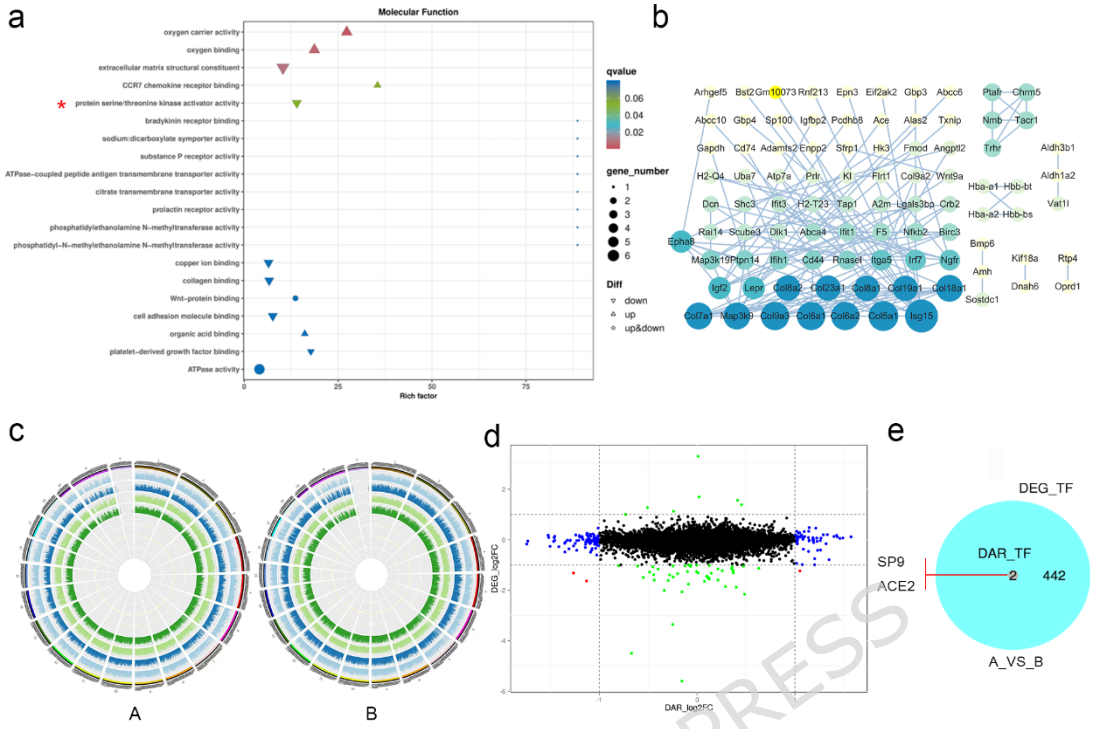


Figure S4. Additional analysis of RNA-seq and RNA-ATAC combined analysis

a. GO enrichment bubble plot of DEGs (molecular function) b. Protein-protein interaction network of DEGs c. Circos plot of ATAC-Seq signal and gene expression data at the chromosomal level. d. Nine-quadrant plot categorizing genes related to differentially accessible regions and differentially expressed genes. e. Venn diagram illustrating overlapping transcription factors enriched in the promoter regions of differentially

ARTICLE IN PRESS

opened regions and differentially expressed genes



ARTICLE IN PRESS